Development of A New Atom-Based SI Traceable Electric-Field Metrology Technique

Christopher L. Holloway, Matt T. Simons, and Joshua A. Gordon
RF Technology Division
National Institute of Standards and Technology (NIST), Boulder, CO 80305
holloway@boulder.nist.gov : 303-497-6184

***Abstract*—We are developing a fundamentally new atom-based approach for electric (E) field metrology. This technique has the capability of becoming a new international standard for E-field measurements and calibrations. Since this new approach is based on atomic transitions of alkali atoms (mainly caesium and rubidium atoms), the probe is self-calibrating and has a capability of performing measurements over a large bandwidth (from 10's MHz to the THz range). This new approach will lead to a self-calibrated, SI traceable, E-field measurement, and has the capability to perform measurements on a fine spatial resolution in both the far-field and near-field. We will report on the development of this new metrology approach, including the first fiber-coupled vapor-cell for E-field measurements, which allows for easier and more flexible measurements. We discuss key applications, including self-calibrated measurements, millimeter-wave and sub-THz measurements, field mapping, and sub-wavelength and near-field imaging. We show results for free-space measurements of E-fields, for measuring the E-field distribution along the surface of a circuit board, and for measuring the directivity pattern of a horn antenna.**

I. Introduction

One of the keys to developing new technologies is to have sound metrology tools and techniques. Whenever possible, we would like these metrology techniques to make absolute measurements of a physical quantity. Preferably, we would like to make measurements directly traceable to the International System of Units (SI). Measurements based on atoms provide such a direct SI traceability path and enable absolute measurements of physical quantities. Atom-based measurements have been used for several years; most notable are time (s), frequency (Hz), and length (m). We would like to extend these atom-based techniques to other physical quantities, including electric (E) fields.

We are developing a fundamentally new atom-based approach that will lead to a self-calibrated, SI traceable E-field measurement that has the capability to perform measurements on a fine spatial resolution in both the far-field and near-field [1]-[9]. This new approach is significantly different from currently used field measurement techniques in that it is based on the interaction of radio-frequency (RF) E-fields with Rydberg atoms (alkali atoms placed in a glass vapor-cell that are excited optically to Rydberg states). The Rydberg atoms act like an RF-to-optical transducer, converting an RF E-field strength to an optical-frequency response. In this new approach, we employ the phenomena of electromagnetically induced transparency (EIT) and Autler-Townes splitting [1]-[3], [10]-[13]. This splitting is easily measured and is directly proportional to the applied RF E-field amplitude and results in an absolute SI traceable measurement. The technique is very broadband allowing self-calibrated measurements over a large frequency band including 500 MHz to 500 GHz (and possibly up to 1 THz and down to 10's of megahertz). Various other benefits of the new approach are listed in [1] and [2].

Besides having a self-calibrating, SI-traceable probe, various other applications are possible, including millimeter-wave and sub-THz measurements, field mapping and sub-wavelength imaging, and far-field and near-field measurements. This technique is demonstrated by showing free-space measurements of E-fields, measurements of the E-field distribution along the surface of a circuit board, and measurements of the directivity pattern of a horn antenna. Some of the measurements presented here are performed with a new fiber-coupled probe. This fiber-coupled design allows for a moveable form-factor probe which makes measurements easier and more flexible for various applications.

II. Description of Technique

The basic concept of this measurement approach uses a vapor of alkali atoms (placed in a glass cell, referred to as a "vapor" cell) as the active medium for the radio frequency (RF) E-field measurement. The basic concept is that by manipulating alkali atoms with both optical (laser) fields and RF fields, it is possible to cause a laser to transmit through a vapor cell where it would normally be absorbed by the atoms in the vapor cell. Rubidium (^{85}Rb) and cesium (^{133}Cs) are the two atomic species that are typically used in the approach.

A typical measurement setup is shown in Fig. 1. This measurement approach can be represented by the four-level atomic system shown in Fig. 2, see [2], [3], [14] for details. In effect, the "probe" laser is used to probe the response of the ground-state transition of the atoms (level 1 to level 2 in Fig. 2), and a second laser ("coupling" laser) is used to excite the atoms to a high energy Rydberg state (level 3 in Fig. 2). In the presence of the coupling laser, a destructive quantum interference occurs and the atoms become transparent to the resonant probe laser (this is the concept of EIT). A transparency window is opened for the probe laser light: probe light transmission is increased. The coupling laser wavelength

(a) photos of setup

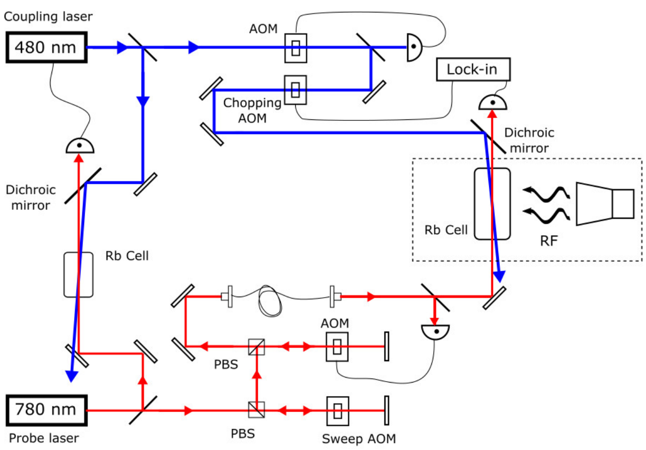

(b) block diagram

Fig. 1. Experimental setup for E-field measurements using EIT: a) photo of of the setup and (b) block diagram, polarizing beam splitter (PBS) and acousto-optic modulator (AOM).

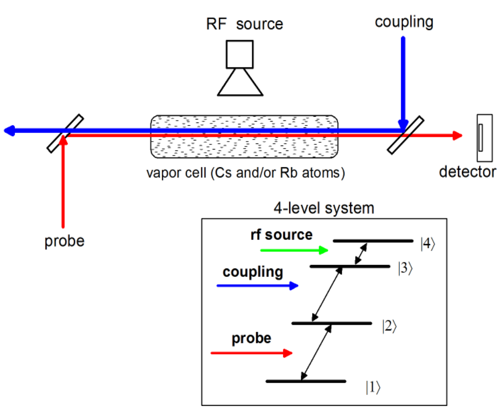

Fig. 2. Illustration of a four-level system, and the vapor cell setup for measuring EIT, with counter-propagating probe and coupling beams. The RF is applied transverse to the optical beam propagation in the vapor cell.

is chosen such that the atom is in a sufficiently high state (a Rydberg state) such that a RF field couples two Rydberg states (levels 3 and 4 in Fig. 2).

A detailed explanation both from an atomic physics viewpoint and experimental approach is given in [1] and [2]. Experimentally, the approach is explained as follows: If the probe laser is tuned to a ground state transition of alkali atoms in a vapor cell (levels 1 and 2 in Fig. 2), after propagation through the vapor cell the atoms will absorb the light and little power will be detected. The power measured on the detector when the laser is scanned across this wavelength is shown in the bottom curve in Fig. 3(a) ($\Delta p = \omega_o - \omega_p$; ω_o is the on-resonance angular frequency of the ground state transition and ω_p is the angular frequency of the probe laser.) This is the typical signal one obtains when performing atomic spectroscopy experiments (i.e., the classical Doppler profile). The minimum in the curve indicates the resonance frequency of the ground state transition of the alkali atom. When the coupling laser is allowed to propagate through the cell (the coupling laser is counter-propagating on top of the probe laser) an interference between the two atomic states occurs, hence allowing the probe laser to pass through the vapor cell with less absorption (an increase in the probe laser transmission). This is the concept of EIT, i.e., a medium that was normally absorbing becomes transparent with the presence of the coupling laser. This is shown in the top curve in Fig. 3(a) (note the wings of all three curves normally would lay on top of one another, but they are shifted here for ease of viewing). Notice at $\Delta_p = 0$, the power on the detector is larger than the Doppler background, i.e., the global inverted bell-shaped behavior. The wavelength of the coupling laser is chosen judiciously such that the atoms are excited to a very high energy, where an RF source is at a resonant frequency that causes an atomic transition to a nearby state (i.e., an RF atomic transition). When the RF source is turned on, the EIT signal splits into two (this splitting is called Autler-Townes (AT) splitting), see the middle curve in Fig. 3(a). The EIT signal and the splitting can be weak at times. To increase the EIT signal-to-noise, we modulate the coupling-laser amplitude with a 50/50 duty-cycle 30 kHz square wave and detect any resulting modulation of the probe transmission with a lock-in amplifier. This removes the Doppler background and isolates the EIT signal. Fig. 3(b) shows a typical EIT signal from the lock-in amplifier. The splitting of the EIT peak is indicated by Δf_m.

This splitting (Δf_m) of the probe laser spectrum is easily measured and is directly proportional to the applied RF E-field amplitude. Once this Δf_m is measured, the RF E-field strength is obtained by [2], [3], [4]:

$$|E| = 2\pi \frac{\hbar}{\wp} \frac{\lambda_p}{\lambda_c} \Delta f_m = 2\pi \frac{\hbar}{\wp} \Delta f_o \ , \tag{1}$$

where $\hbar$ is Planck's constant, $\wp$ is the atomic dipole moment of the RF atomic transition (see [2]), $\Delta f_o = \frac{\lambda_p}{\lambda_c} \Delta f_m$, and λ_p and λ_c are the wavelengths of the probe and coupling laser, respectively. The λ_p/λ_c ratio is needed to account for the Doppler mismatch of the probe and coupling lasers [10], when the probe laser is scanned during the experiments. One can also scan the coupling laser and not the probe laser during the experiments. If the coupling laser is scanned, it is not required to correct for the Doppler mismatch, and λ_p/λ_c ratio is not needed, see [14] for details. In this case, $\Delta f_o = \Delta f_m$.

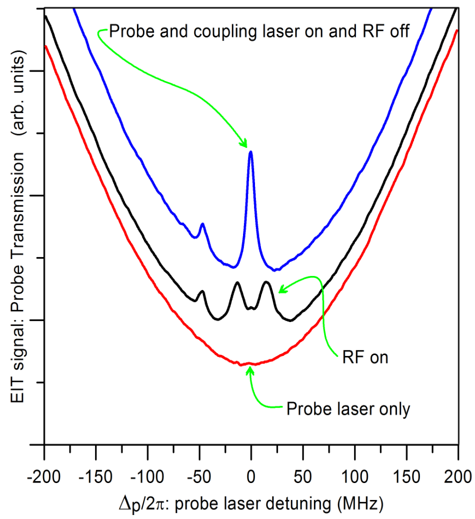

(a)

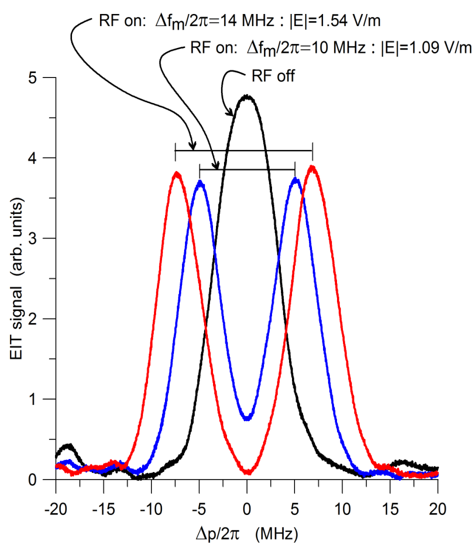

(b)

Fig. 3. EIT illustration: (a) with the Doppler ground and (b) after the lock-in is used. These experiments where performed with a vapor cell filled with ^{133}Cs and with a RF source at 9.22 GHz. The RF source couples Rydberg states 43D$_{5/2}$-44P$_{3/2}$ for the E-field measurement.

We consider this type of measurement of the E-field strength a direct SI-traceable, self-calibrated measurement in that it is related to Planck's constant (which will become an SI-defined quantity by standard bodies in the near future) and only requires a frequency measurement (Δf_m, which is quantum linked and can be measured very accurately). The one unknown in the expression is the atomic dipole moment $\wp$ which can be calculated accurately, see [2], [15], [16].

Fig. 3(b) shows the measured EIT signal for three different RF incident field strengths (0 V/m, 1.09 V/m and 1.54 V/m). In order to estimate the E-field strength, we first measured Δf_m, then we used eq. (1) to determine $|E|$.

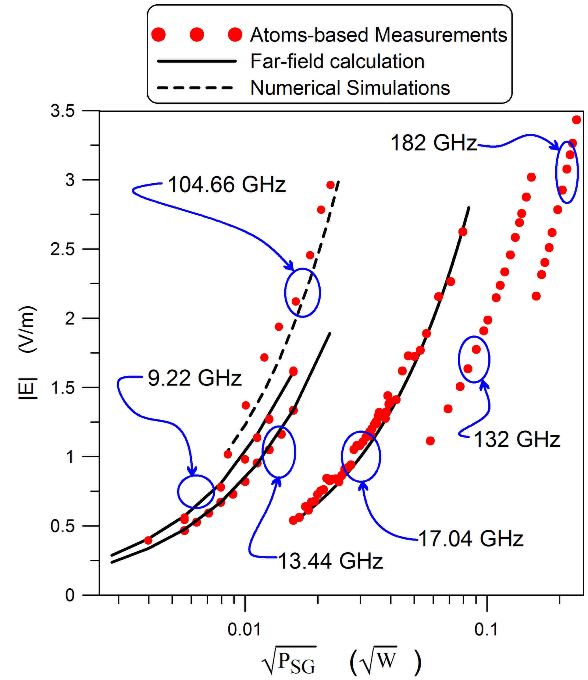

Fig. 4. A comparison of the measured E-field (obtained from the atom-based approach) to results obtained from far-field calculations and from a full-wave numerical simulation. Comparing experimental atom-based data to both numerical simulations and to far-field calculations for various frequencies from 9 GHz to 182 GHz helps to validate this technique. PSG is the signal-generator power level feeding the antennas (through either a cable or a waveguide). Note that a log scale is used because the data sets cover different $\sqrt{P_{SG}}$ ranges.

III. Experimental Results

A. Far-field Comparisons

Utilizing the experiment setup shown in Fig. 1 we can measure the E-field strength in the far-field at various frequencies. Fig. 4 shows measurement for six different frequencies ranging from 9.22 GHz to 182 GHz using two different atomic species (^{85}Rb and ^{133}Cs). In this figure we have compared the estimated E-field obtained for this atom-based approach to both far-field calculations and to numerical simulations. We see that the atom-based approach correlates very well to both the far-field calculations and to numerical simulations.

These results show the wide bandwidth measurement capacity of this approach. With one experimental setup, it is possible to measure E-field strength from 10's MHz into the THz frequency range. Measurements above 110 GHz have been demonstrated here and in [1], [5]. The possibility of performing calibrated measurements above 110 GHz is one of the interesting and possibly, one of the major benefits of this new technique, since it can provide calibration above 110 GHz (which is currently not possible).

B. Movable Probe: Fiber Coupled Probe

While various international metrology organizations groups around the world are beginning to investigate this new approach as a possible new international standard for E-field

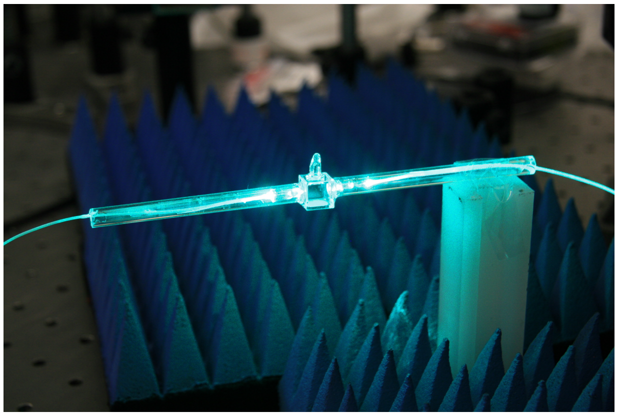

Fig. 5. Photo of first fiber-coupled vapor cell probe for self-calibrated E-field measurements over a large frequency band including 500 MHz to 500 GHz (and possibly up to 1 THz and down to tens of megahertz).

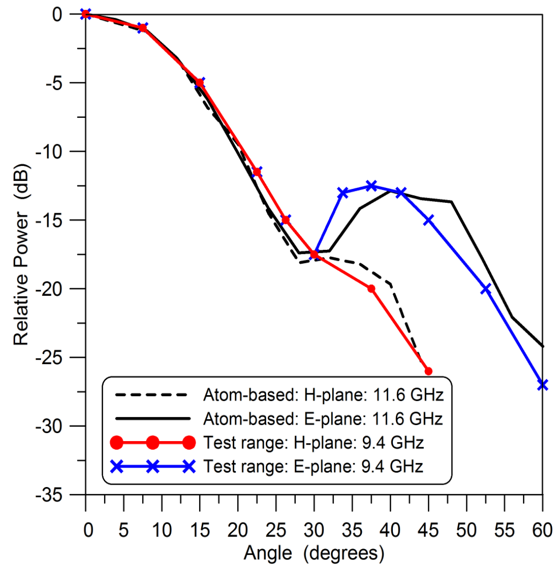

Fig. 6. Fiber-coupled probe measurement for the E-plane and H-plane antenna pattern for a Narda 640 standard gain horn at 11.6 GHz. Also shown are measured results obtained from an antenna range [17] at 9.4 GHz.

measurements and calibrations, all these investigations and measurements have been confined to an optical table. This confinement is a result of the fact that this technique requires the two lasers (probe and coupling laser) to overlap inside the vapor cell. In order to overcome these issues, we have developed the first fiber-coupled vapor cell, where the counter propagating probe and pump fields are overlapped inside the vapor cell while it is moved off the optical bench. Moving the probe off the optical table allows measurements to be performed in free space, and in other standard RF metrology environments. The new probe consists of a 10-mm cubic vapor cell filled with ^{133}Cs and two optical fibers with lenses attached with UV curing epoxy at either end, made with all dielectric material (see Fig. 5). We have performed various types of measurement in order to illustrate its capability.

1) Antenna Pattern Measurements: We used the fiber-coupled probe to measure the antenna pattern for a Narda 640 standard gain horn antenna (mentioning this product does not imply an endorsement, but serves to clarify the antenna used). In these measurements, the fiber-coupled probe was placed in the far-field of the horn antenna and scanned from bore-site to an angle of 60^o. The horn antenna was scanned in both E-plane and H-plane. Fig. 6 shows the measured antenna patterns for both the E-plane and H-plane at 11.6 GHz. Also shown in this figure are results obtained in an anechoic chamber test range [17] at 9.4 GHz. Good correlation between the two types of measurements is seen. The deviations to the two sets of measurements is due to the fact that our measurement were perform in a laboratory with no RF absorber on the walls and the laboratory had several objects in the room. Thus, our results suffer from some background scattering.

2) Near-Field Imaging: In order to illustrate the near-field imaging capability of the fiber-coupled probe, we imaged the E-field at various heights across the surface of a co-planar waveguide (CPW) line. The CPW has a center strip of 3 mm, gaps of 2 mm, and a substrate ($\epsilon_r \approx 3.5$) of thickness 1.52 mm. Fig. 7 shows the scans at six different heights for a frequency of 11.6 GHz. In order to show the repeatability of this probe we performed three sets of measurements for each height and the error-bars represent all these measurements. These results show the capability for near-field imaging and field-mapping across the surface of printed circuit board structures, which will be used in the future to support calibrated on-wafer measurements of high-speed (high-frequency) integrated circuits. The fiber-coupled probe allows for much finer spatial resolution than is possible with current E-field probes.

IV. Measurement Uncertainties

Knowing the uncertainties of this technique is an important step when establishing a new international measurement standard for an E-field strength and is a necessary step for this method to be accepted as a standard calibration technique. The uncertainties can be grouped into two different categories: (a) quantum based uncertainties and (b) RF based uncertainties. These include, 1) the validity of eq. (1), 2) the accuracy of the atomic dipole moment calculation, and 3) perturbation of the RF field due to internal resonances inside the vapor cell, just to name a few. These three and other various types of uncertainties for this atom-based approach are currently being investigated [1], [3], [7], [14], [18], [19]. The uncertainties of this new atom-based technique can be controlled and reduced to be less than the current E-field measurement uncertainties. In the near future we will develop detailed uncertainties for this new approach.

V. Conclusion

We discussed a fundamentally new atom-based approach for E-field metrology. Several international metrology organizations around the world are beginning to investigate this new approach as a possible new international standard for E-field measurements and calibrations. In this paper we have presented some key examples that show the benefits

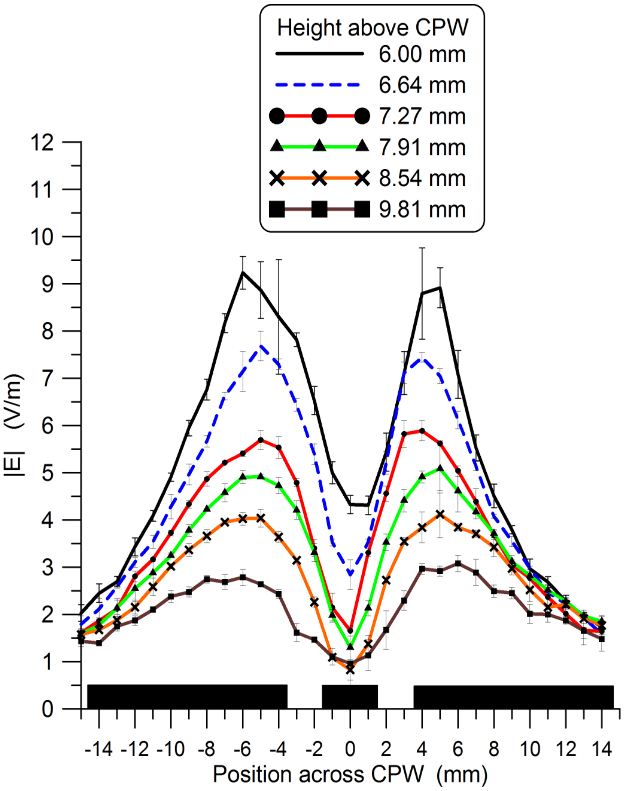

Fig. 7. Measured $|E|$-field distribution across the surface of the CPW line at different heights for 11.6 GHz obtained with the fiber-coupled probe. We also show the CPW geometry in order to illustrate the gap locations.

of the new approach and that show the potential for a new international measurement standard. We have shown results for far-field measurement, results for the broadband nature of this technique, results of antenna pattern measurements, and results of near-field imaging. The fiber-coupled probe is one important advancement of this approach. That is, being able to move the probe off the optical table is an important step when establishing a new international measurement standard for an E-field strength and is a necessary step for this method to be useful and ultimately accepted as a standard calibration technique.

References

[1] C.L. Holloway, M.T. Simons, J.A. Gordon, P.F. Wilson, C.M. Cooke, D.A. Anderson, and G. Raithel, "Atom-Based RF Electric Field Metrology: From Self-Calibrated Measurements to Sub-Wavelength and Near-Field Imaging", *IEEE Trans. on Electromagnetic Compat.,* vol. 59, no. 2, 717-728, 2017.

[2] C.L. Holloway, J.A. Gordon, A. Schwarzkopf, D. A. Anderson, S. A. Miller, N. Thaicharoen, and G. Raithel, "Broadband Rydberg Atom-Based Electric-Field Probe for SI-Traceable, Self-Calibrated Measurements," *IEEE Trans. on Antenna and Propag.*, vol. 62, no. 12, 6169-6182, 2014.

[3] J.A. Sedlacek, A. Schwettmann, H. Kübler, R. Löw, T. Pfau and J. P. Shaffer, 'Microwave electrometry with Rydberg atoms in a vapor cell using bright atomic resonances", *Nature Phys.*, vol. 8, 819, 2012.

[4] C.L. Holloway, J.A. Gordon, A. Schwarzkopf, D.A. Anderson, S.A. Miller, N. Thaicharoen, and G. Raithel, "Sub-wavelength imaging and field mapping via electromagnetically induced transparency and Autler-Townes splitting in Rydberg atoms," *Applied Phys. Lett.,* vol. 105, 244102, 2014.

[5] J.A. Gordon, C.L. Holloway, A. Schwarzkopf, D.A. Anderson, S.A. Miller, N. Thaicharoen, and G. Raithel, "Millimeter-wave detection via Autler-Townes splitting in rubidium Rydberg atoms", *Applied Phys. Lett.*, vol. 105, 024104, 2014.

[6] J.A. Sedlacek, A. Schwettmann, H. Kübler, and J.P. Shaffer, "Atom-based vector microwave electrometry using rubidium Rydberg atoms in a vapor cell," *Phys. Rev. Lett.*, vol. 111, 063001, 2013.

[7] H. Fan, S. Kumar, J. Sedlacek, H. Kübler, S. Karimkashi, and J.P. Shaffer, 'Atom based RF electric field sensing," *J. of Phys. B: Atomic, Molecular and Optical Physics*, vol. 48, 202001, 2015.

[8] M. Tanasittikosol, J.D. Pritchard, D. Maxwell, A. Gauguet, K.J. Weatherill, R.M. Potvliege and C.S. Adams, "Microwave dressing of Rydberg dark states," *J. Phys B*, vol. 44, 184020, 2011.

[9] C.G. Wade, N. Sibalic, N.R. de Melo, J.M. Kondo, C.S. Adams, and K.J. Weatherill, "Real-Time Near-Field Terahertz Imaging with Atomic Optical Fluorescence," *Nature Photonics,* **11**, 40-43, 2017.

[10] A.K. Mohapatra, T.R. Jackson, and C.S. Adams, "Coherent optical detection of highly excited Rydberg states using electromagnetically induced transparency," *Phys. Rev. Lett.*, vol. 98, 113003, 2007.

[11] M. Fleischhauer, A. Imamoglu, and J.P. Marangos, "Electromagnetically induced transparency: Optics in coherent media," *Reviews Modern Physics*, vol. 77, pp. 633-673, April, 2005.

[12] K.J. Boller, A. Imamolu, and S.E. Harris, "Observation of electromagnetically induced transparency," *Phys. Rev. Lett.*, vol. 66, no. 20, pp. 2593-2596, May, 1991.

[13] S.H. Aulter and C.H. Townes, "Stark Effect in Rapidly Varying Fields," *Phys. Rev.*, vol. 100, 703-722, October, 1955.

[14] C.L. Holloway, M.A. Simons, J.A. Gordon, A. Dienstfrey, D.A. Anderson, and G. Raithel, "Electric Field Metrology for SI Traceability: Systematic Measurement Uncertainties in Electromagnetically Induced Transparency in Atomic Vapor", *J. of Applied Physics*, vol. 121, 233106, 2017.

[15] I.I. Sobelman, *Atomic Spectra and Radiative Transitions*, (Second Edition): Springer, 1992.

[16] M.A. Simons, J.A. Gordon, and C.L. Holloway, "Simultaneous Use of Cs and Rb Rydberg Atoms for Dipole Moment Assessment and RF Electric Field Measurements via Electromagnetically Induced Transparency", *J. Appl. Phys.*, vol. 102, 123103, 2016.

[17] T.J. Duck, B. Firanski, F.D. Lind, and D. Sipler, "Aircraft-protection radar for use with atmospheric lidars", *Applied Optics*, vol. 44, no. 23, pp. 4937-4945, 2005.

[18] H. Fan, S. Kumar, J. Sheng, J.P. Shaffer, C.L. Holloway and J.A. Gordon, "Effect of Vapor Cell Geometry on Rydberg Atom-based Radio-frequency Electric Field Measurements", *Physical Review Applied*, vol. 4, 044015, November, 2015.

[19] C.L. Holloway, J.A. Gordon, M.T. Simons, H. Fan, S. Kumar, J.P. Shaffer, D.A. Anderson, A. Schwarzkopf, S. A. Miller, N. Thaicharoen, and G. Raithel, "Atom-based RF electric field measurements: an initial investigation of the measurement uncertainties," in Proc. of *Joint IEEE Intern. Symp. on EM and EMC Europe*, Dresden, Germany, pp. 467-472, Aug. 2015.